PROCEEDINGS OF SCIENCE

Experiments on photon-induced reactions for p-process nucleosynthesis*

K. Sonnabend†, S. Müller, N. Pietralla, D. Savran, L. Schnorrenberger
Institut für Kernphysik, Technische Universität Darmstadt, Schlossgartenstraße 9, D-64289 Darmstadt, Germany
E-mail: sonnabend@ikp.tu-darmstadt.de

J. Hasper, A. Zilges
Institut für Kernphysik, Universität zu Köln, Zülpicher Str. 77, D-50937 Köln, Germany

Photodesintegration rates – like (γ,n), (γ,p), and (γ,α) – play an important role in the nucleosynthesis of the so-called *p* nuclei. These proton-rich, in general very low-abundant isotopes cannot be produced by neutron capture reactions. Experiments using continuous-energy bremsstrahlung and the activation technique are perfectly suited to carry out systematic surveys on (γ,n) reactions. In addition, single cases can be studied in more detail using energy-resolved methods as provided by photon sources based on the principle of Laser-Compton backscattering or photon tagging. An overview about current results on photon-induced reactions and recent instrumental developments is given.

10th Symposium on Nuclei in the Cosmos
July 27 - August 1, 2008
Mackinac Island, Michigan, USA

*This work was supported by Deutsche Forschungsgemeinschaft (contract SFB 634).
†Speaker.

1. Introduction

The heavy elements above the so-called iron peak are mainly produced in neutron capture processes. Two different scenarios account for the observed double-peak structure in the solar abundance distribution. The *r* process (*r*: rapid neutron capture) deals with high neutron densities well above 10^{20} cm^{-3} and temperatures in the order of $2-3 \cdot 10^9$ K. It is thought to occur in explosive scenarios like *e.g.* supernovae and is responsible for the broad peaks around the mass numbers $A \approx 80, 130, 190$, respectively [1, 2].

The sharper peaks at higher mass numbers are due to *s*-process nucleosynthesis. There are different sites proposed for the *s* process to occur. During stellar burning of massive stars with $M \approx 10\ M_\odot$ the weak *s* component is produced during He-core burning ($T \approx 3 \cdot 10^8$ K, $n_n < 10^6$ cm^{-3}, neutron source: ^{22}Ne(α,n)^{25}Mg) and in the C-shell burning phase ($T \approx 10^9$ K, $n_n \approx 10^{11}$ cm^{-3}, neutron source: ^{12}C(^{12}C,n)^{23}Mg). The main component is synthesized in asymptotic giant branch (AGB) stars with masses $M \approx 1-3\ M_\odot$. This site is characterized by the alternating action of two neutron sources which are the reactions ^{13}C(α,n)^{16}O ($T \approx 9 \cdot 10^7$ K, $n_n \approx 10^7$ cm^{-3}) during the H-burning episodes and ^{22}Ne(α,n)^{25}Mg ($T \approx 2.5 \cdot 10^8$ K, $n_n \approx 10^{11}$ cm^{-3}) during the recursive He-shell flashes [3, 4, 5].

The average neutron densities are rather small ($n_n \approx 10^8$ cm^{-3}), *i.e.* the neutron capture rate λ_n is normally well below the β-decay rate λ_β and the reaction path is close to the valley of β stability. However, during the peak neutron densities branchings occur at unstable isotopes with half-lives as low as several days. The branching ratio λ_β/λ_n is determined by the half-life and neutron capture cross section of the branching point nucleus which is the nuclear physics input. However, these properties have to be known under stellar conditions and, thus, are also influenced by the temperature and neutron densitiy occuring at *s*-process nucleosynthesis sites. Due to the fact, that the branching ratio determines the relative isotopic abundances in the following elemental chains the astrophysical parameters can be fixed by the observed abundance ratio if the nuclear physics parameters are known with sufficient uncertainties. While the half-lives of these branching points are normally known with high accuracy at least under laboratory conditions and rely only on theory for the extrapolation to stellar temperatures [6], the neutron capture cross sections are only in special cases accessible to direct experiments. Besides the production of a sufficient amount of target material, the intrinsic activity of the target mainly hinders the experimental access especially in the case of the short-lived branching points.

However, the predictions in the Hauser-Feshbach model yield different results due to the underlying parameter sets. Additionally, the single studies on long-lived branching points (*e.g.* ^{147}Pm [7], ^{151}Sm [8, 9], ^{155}Eu [10]) showed that the recommended values of neutron capture cross sections in the Hauser-Feshbach statistical model [11] differ by up to 50% from the experimentally determined values. Thus, any experimental constraints on the theoretical predictions of these crucial values are welcome. Therefore, the inverse (γ,n) reaction could be used to decide for the most suitable parameter set and to predict a more reliable neutron capture cross section using these input values. This method has been applied to the branching nucleus ^{185}W using a continuous-energy bremsstrahlung spectrum [12] and Laser-Compton backscattered photons [13, 14]. It is also supposed to yield information for the calculation of Stellar Enhancement Factors (SEF) in some special cases like *e.g.* ^{151}Sm [15].

PoS(NIC X)043

The necessity of a precise knowledge of photodissociation cross sections is even more apparently for the production of the so-called p nuclei. These proton-rich isotopes between Se and Hg cannot be synthesized by neutron capture processes and are thought to originate from explosive events lasting a few seconds and delivering temperatures of about $2-3\cdot10^9$ K [16, 17]. In this scenario, s- and r-process seed nuclei are converted to the proton-rich side of the valley of stability by a series of (γ,n), (γ,p), and (γ,α) reactions. However, the light p nuclei, like *e.g.* ^{92,94}Mo and ^{96,98}Ru, are significantly underproduced in the models describing this process sometimes referred to as γ process [17].

The efforts to solve this problem include alternative processes of nucleosynthesis, like *e.g.* the rp process [18] or the νp process [19], as well as suggestions of revised cross section data, like *e.g.* an enhanced ^{22}Ne(α,n) cross section leading to an increase of the s-process seed [20]. On that score, the knowledge about photodissociation cross sections plays a crucial role in the prediction of the abundances of the p nuclei.

We describe in section 2 how the activation technique is applied to study photon-induced reactions for p-process nucleosynthesis and discuss pros and cons. Section 3 focusses on the usage of tagged photons while alternative methods to study also unstable isotopes are addressed in the concluding section 4.

2. Photoactivation experiments

At the High Intensity Photon Setup (HIPS) of the S–DALINAC [21, 22] continuous-energy bremsstrahlung is produced by fully stopping the monoenergetic electron beam in a thick radiator target of copper. Due to the high currents of up to 40 μA, the photon intensity reaches maximum values of about 10^7 keV^{-1} s^{-1} cm^{-2} at 80% of the maximum energy E_{max}. If experiments are carried out at different energies it is possible to calculate the ground-state reaction rates of (γ,n) reactions at typical p-process temperatures of about $2-3\cdot10^9$ K from the experimental data without any assumption on the energy dependence of the photodissociation cross section. This method was explained in detail in [23] and results on systematic surveys in the rare earth region [24] and the Pt-to-Pb region [25] were presented.

Figure 1 shows a summary of these results. The experimentally determined reaction rate λ_{exp} is compared to the theoretical value λ_{theo} calculated from the cross section predicted by the NON-SMOKER$^{\mathrm{WEB}}$ code [26] and the TALYS code [27] and the ratio is plotted as function of mass number A. Although no systematic deviation can be observed, the discrepancy between theory and experiment is more than a factor of 2 for single isotopes. The advantages of this method are that the temperature of the underlying Planck distribution can be changed offline by re-adjusting the weighting factors and that any resonance structure of the cross section is included because the analysis does not depend on the prediction of a (γ,n) cross section.

In general, the photoactivation technique is perfectly suited to carry out such systematic surveys: due to the determination of the activation yield in a low-background environment using high-resolution γ spectroscopy with HPGe detectors and/or low-energy photon spectrometers (LEPS) naturally composed targets can be used and several isotopes are measureable in one activation (*e.g.* ^{196}Hg, ^{198}Hg, ^{199m}Hg, ^{200}Hg). Also very weak signatures of the decay of the produced unstable isotopes are analyzable with reasonable statistical uncertainties (*e.g.* ^{185}W: $T_{1/2}=75$ d, $E_\gamma=125$ keV,

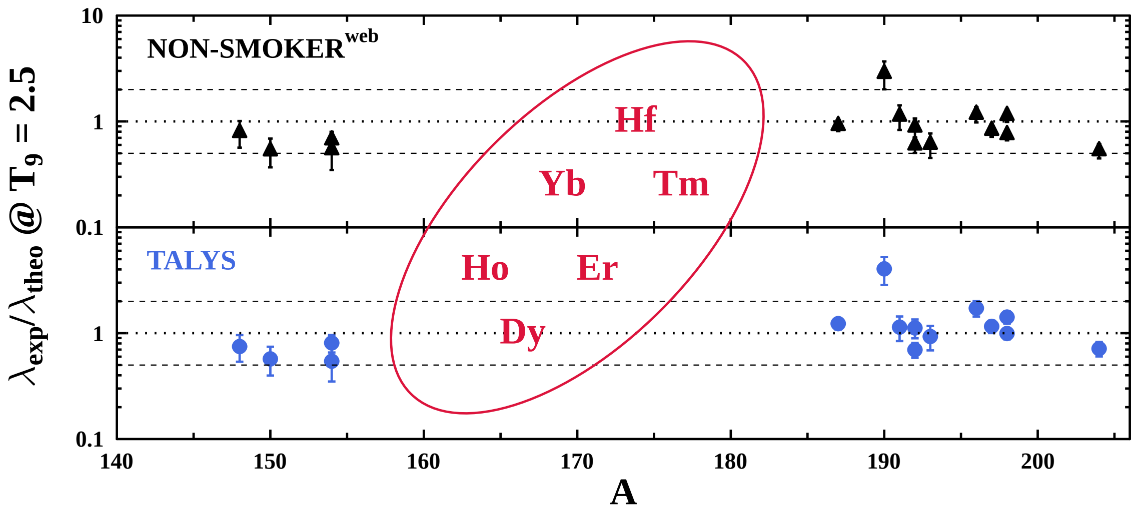

Figure 1: Ratio of groundstate reaction rates. The groundstate reaction rates of several isotopes at a typical *p*-process temperature of $T = 2.5 \times 10^9$ K derived with the superposition method at the S–DALINAC are compared to theoretical predictions in the NON-SMOKER$^{\text{WEB}}$ code [26] and the TALYS code [27]. No systematic deviation was observed although discrepancies of more than a factor of 2 occur [24]. The indicated Dy-to-Hf region was observed at HIPS, Darmstadt, to complete the systematic survey in the shown mass region but the analysis is still in progress.

$I_\gamma = 1.92 \cdot 10^{-4}$). Additionally, the high intensity of continuous-energy bremsstrahlung allows the simultanuous activation of several targets (*e.g.* Dy, Ho, Er, Yb, Tm, and Hf).

However, problems occur if the life-time of the produced nuclei is too long and/or the γ transitions in their decay are too weak to be observable with γ spectroscopy. Alternatively, the reaction yield can be determined by accelerator mass spectrometry (AMS) as proven *e.g.* in the study of the neutron capture cross sections of ^{58}Ni and ^{78}Se [28]. But this technique is not a standard method in the mass region of interest, *i.e.* intense studies and instrumental developments are required for each single case.

Another problem arises if energy-resoluted data is needed. Using continuous-energy bremsstrahlung one needs to calculate the difference of two measurements with maximum photon energies of $E_{\max,1}$ and $E_{\max,2}$. To yield a good energy resolution the difference between $\text{E}_{\max,1}$ and $\text{E}_{\max,2}$ has to be small and, thus, differences between nearly similar numbers have to be calculated during the analysis resulting in quite large uncertainties. This problem can be avoided if the initial photon distribution is already restricted to a more narrow energy region as provided by sources using the principle of Laser-Compton backscattered photons as *e.g.* the High Intensity Gamma Source (HIγS) at DFELL, Duke University, U.S.A. [29] or AIST, Tsukuba, Japan [30]. In a recent experiment on the activation of naturally composed Zr and Ce targets, the intensities of HIγS were proven to be high enough to get reasonable activation yields after irradiations of only a couple of hours [31].

However, the energy resolution of these facilities is still limited to values in the order of 100 keV. Thus, to measure the energy dependence of photodissociation cross section with better accuracy – especially if the astrophysically relevant energy region is close to the reaction threshold as in the case of (γ,n) reactions – tagged photons can be used. The NEPTUN tagger setup at the S–DALINAC, Darmstadt, [32, 33] that is described in more detail in the following paragraph will be suitable for such high resolution studies.

3. Experiments with tagged photons

Using tagged photons it is possible to directly determine the energy dependence of the cross section $\sigma(E_\gamma)$ of a photodissociation reaction (γ,X) where X stands for neutrons, protons, or α particles. The monoenergetic electron beam hits a very thin radiator target in order to ensure that each electron produces at most one photon. The inelastically scattered electrons are deflected onto a focal plane detector consisting of small scintillation fibers using a homogenuous magnetic field. Therefore, the position of the hitted detector in the focal plane is related to the momentum of the scattered electron p_e and determines its energy E_e. The energy of each produced photon E_γ can be calculated as the difference between the energy of the scattered electron E_e and the incident beam energy E_i:

$$E_\gamma = E_i - E_e. \tag{3.1}$$

By applying a coincidence between the focal plane detectors and the (γ,X) reaction products the incoming photons are tagged with their energy information and the reaction cross section can be measured as a function of energy. The energy resolution that can be achieved at a tagging system corresponds directly to the energy resolution of the used electron beam, the granularity of the focal plane, and the focussing characteristics of the magnet. The NEPTUN tagger setup at the S–DALINAC, Darmstadt, is designed for a photon energy range of 6 to 20 MeV which is perfectly suited for photodissociation experiments with astrophysical motivation. The planned energy resolution of 25 keV at a photon energy of 10 MeV was nearly achieved in first test experiments: A HPGe detector was placed into the photon beam at the future experimental position. The untagged spectrum (upper part of Fig. 2) shows the measured continuous-energy bremsstrahlung spectrum folded with the detector response. In the lower parts of Fig. 2 the spectra derived by measuring in coincidence to three different scintillation fibers, *i.e.* three different photon energies, are shown. Photo-peak, single-escape peak and Compton-background are clearly visible while the double-escape peak has only poor statistics.

As a measure for the energy resolution the full-width-at-half-maximum (FWHM) of the photo-peak was derived of such spectra. Measurements with different incident electron energies and different settings of the magnetic field yield to tagged photon energies between about 2 and 12 MeV. A mean value of (34.2 ± 1.7) keV was received as shown in Fig. 3 (compare L. Schnorrenberger, this volume). As an upgrade, the focal plane is extended of 32 to 128 plastic scintillation fibers to enlarge the energy range covered with one magnetic field to about 3 MeV.

The detector array for experiments on (γ,n) reactions will consist of fourteen standard liquid scintillator detectors and applied pulse shape analysis for the photon-to-neutron discrimination. To measure neutrons with very low energies emitted just above the reaction threshold four liquid scintillators enriched in ^{10}B will be added in which the reaction ^{10}B(n,α)^{7}Li provides an additional signature for the discrimination of photons and neutrons. Amendments with other detector types – such as Li glass detectors – will also be tested.

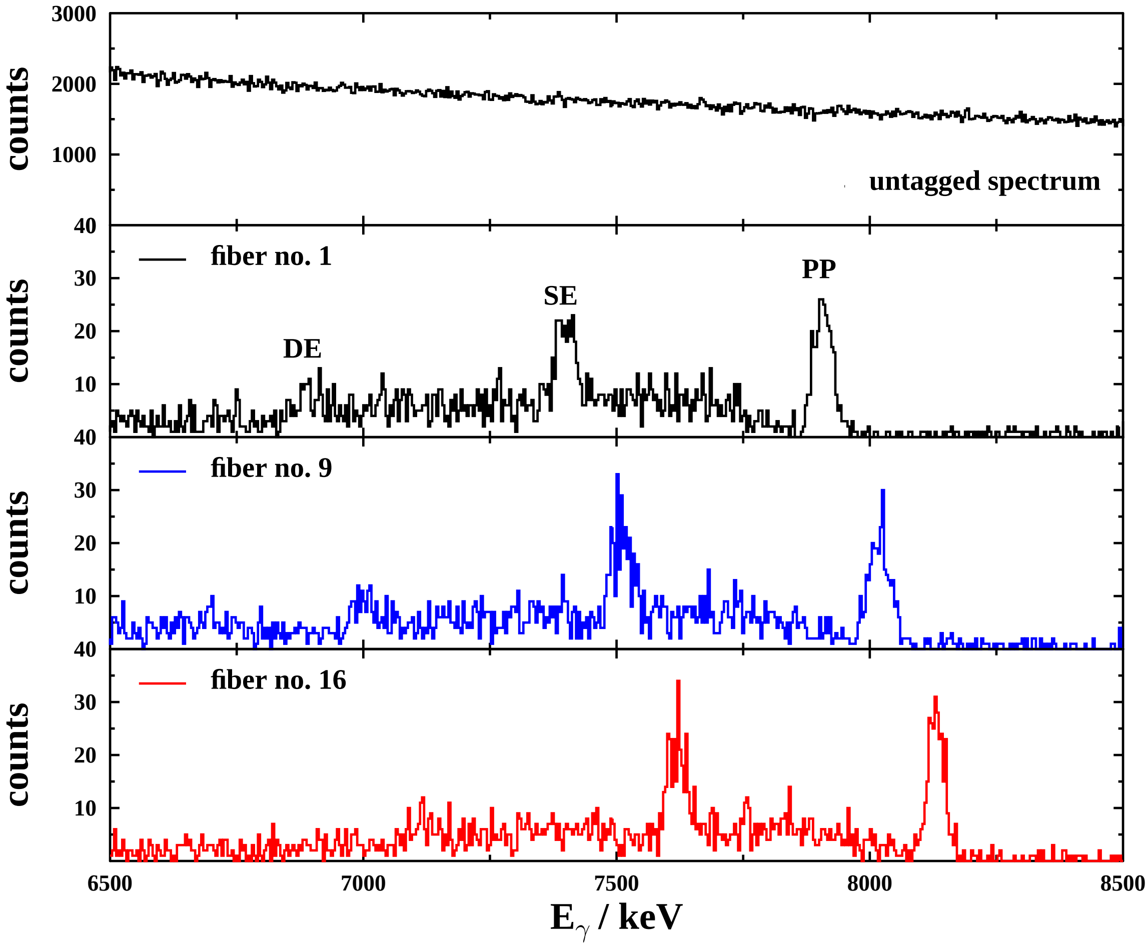

Figure 2: Results of first test experiments at the photon tagger NEPTUN, Darmstadt. A HPGe detector was placed into the photon beam at the future experimental position. The upper part shows the untagged spectrum. In the lower parts, the spectra derived by measuring in coincidence to the scintillation fibers 1, 9, and 16, respectively, are shown. They correspond to the typical detector response of a HPGe detector to a photon beam with a small energy spread: the photo-peak (PP) at the energy of the photons E_γ, the single-escape peak (SE) at $E_\gamma - 511$ keV and the continuous Compton-scattered background. The double-escape peak (DE) at $E_\gamma - 1022$ keV has only poor statistics and, thus, is not clearly visible.

The granularity of this detector array will help to determine the angular distribution of the emitted neutrons. Combined with a precise determination of the neutron energy by time-of-flight (TOF) measurements it will be possible to distinguish between decay channels to the ground and excited states of the resulting nuclei with the resolution provided by the tagging system. The construction of the array for particle detection that is needed to measure (γ,p) and (γ, α) reactions is in the initial phase of simulations. Recently, (γ,α) reactions were also studied successsfully using continuous-energy bremsstrahlung at Forschungszentrum Dresden (see [34] and C. Nair, this volume).

PoS(NIC X)043

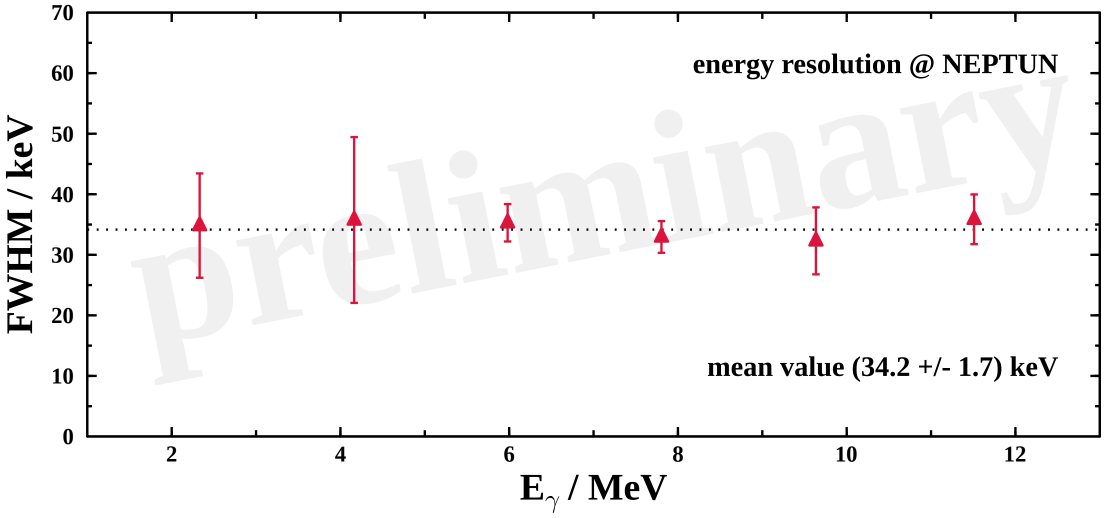

Figure 3: Energy resolution at the photon tagger NEPTUN, Darmstadt. In spectra similar to those shown in the lower part of Fig. 2 the full-width-at-half-maximum (FWHM) of the photopeak was determined. This value is a measure for the energy resolution of the tagging facility and is plotted as a function of the tagged photon energy. The weighted mean is (34.2 ± 1.7) keV which is already close to the design value of 25 keV.

4. Conclusions and Outlook

The sensitivity of the activation technique enables to measure reaction rates even though low reaction yields are expected due to low cross sections and/or low amounts of target material *i.e.* this technique is perfectly suited to carry out systematic surveys in broad mass ranges. Instead of continuous-energy bremsstrahlung other photon sources using the principles of Laser-Compton backscattering or photon tagging are useful to study single cases in more detail by an energy-resolved experiment. However, these methods are limited to the observation of stable isotopes while the interesting cases of *p*-process nucleosynthesis are proton-rich unstable nuclei where (γ,p) and (γ,α) reactions compete with the formerly dominating (γ,n) reactions (compare [35, 36]).

Experiments using Coulomb Dissociation (CD) in inverse kinematics as feasible at the SIS/FRS/LAND setup at GSI, Darmstadt, [37] can extend the investigations in that direction. A first test was carried out on the (γ,n) cross sections of the isotopes ^{92,93,94,100}Mo [38]. To compare the reliability of the CD method, the cross sections of ^{92}Mo(γ,n)+(γ,p) [39] and ^{100}Mo(γ,n) were observed at the ELBE accelerator at Forschungszentrum Dresden and at the S–DALINAC, Darmstadt, respectively, using continuous-energy bremsstrahlung. The data of the activation experiments is compared to the results of the CD measurements to estimate the influence of several potential complications on the interpretation of data taken in CD experiments. The contribution of nuclear break-up and the fraction of different multiplicities to the cross section have to be taken into account as well as the final-state interactions known as post-Coulomb acceleration to extract a reasonable result of the CD data.

However, besides experiments directly observing photon-induced reactions other approaches aiming in the constraint of theoretical predictions of the corresponding reaction rates are currently of interest. Amongst these are systematic studies on the influence of underlying particle nucleus potentials as for ^{106}Cd [40] and ^{112}Sn [41], observations of α-induced reactions in the corresponding Gamow window [42], and experiments using the inverse (n,γ) reaction [43].

Acknowledgements

We thank the accelerator group of the S–DALINAC around R. Eichhorn for the support during beam-times at HIPS and NEPTUN. We also thank R. Gallino, S. Goriely, F. Käppeler, A. Mengoni, and T. Rauscher for helpful discussions. This work was supported by DFG under contract SFB 634 and partly by BMBF.

References

[1] K.-L. Kratz, J.-P. Bitouzet, F.-K. Thielemann, P. Möller, B. Pfeiffer, Astrophys. J. **403** (1993) 216.

[2] G. Wallerstein, I. Iben, P. Parker, A. M. Boesgaard, G. M. Hale, A. E. Champagne, C. A. Barnes, F. Käppeler, V. V. Smith, R. D. Hoffman, F. X. Timmes, C. Sneden, R. N. Boyd, B. S. Meyer, D. L. Lambert, Rev. Mod. Phys. **69** (1997) 995.

[3] F. Käppeler, Prog. Part. Nucl. Phys. **43** (1999) 419.

[4] F. Käppeler, A. Mengoni, Nucl. Phys. **A777** (2006) 291.

[5] I. Dillmann, C. Domingo Pardo, F. Käppeler, A. Mengoni, K. Sonnabend, Publications of the Astronomical Society of Australia **25** (2008) 18.

[6] K. Takahashi, K. Yokoi, Nucl. Phys. **A404** (1983) 578.

[7] R. Reifarth, C. Arlandini, M. Heil, F. Käppeler, P. V. Sedyshev, A. Mengoni, M. Herman, T. Rauscher, R. Gallino, Astrophys. J. **582** (2003) 1251.

[8] U. Abbondanno, G. Aerts, R. Terlizzi, H. Álvarez, F. Alvarez-Velarde, S. Andriamonje, J. Andrzejewski, P. Assimakopoulos, L. Audouin, G. Badurek, P. Baumann, F. Bečvář, J. Benlliure, E. Berthoumieux, F. Calviño, D. Cano-Ott, R. Capote, A. Carrillo de Albornoz, P. Cennini, V. Chepel, E. Chiaveri, N. Colonna, G. Cortes, D. Cortina, A. Couture, J. Cox, S. David, R. Dolfini, C. Domingo-Pardo, W. Dridi, I. Duran, M. Embid-Segura, L. Ferrant, A. Ferrari, L. Fitzpatrick, R. Ferreira-Marques, H. Frais-Kölbl, K. Fujii, W. Furman, C. Guerrero, I. Goncalves, R. Gallino, E. Gonzalez-Romero, A. Goverdovski, F. Gramegna, E. Griesmayer, F. Gunsing, B. Haas, R. Haight, M. Heil, A. Herrera-Martinez, M. Igashira, S. Isaev, E. Jericha, Y. Kadi, F. Käppeler, D. Karamanis, D. Karadimos, M. Kerveno, V. Ketlerov, P. Koehler, V. Konovalov, E. Kossionides, M. Krtička, C. Lamboudis, H. Leeb, A. Lindote, I. Lopes, M. Lozano, S. Lukic, J. Marganiec, L. Marques, S. Marrone, A. Mastinu, P. Mengoni, , P. M. Milazzo, M. Moreau, C. Mosconi, , F. Neves, H. Oberhummer, S. O'Brien, M. Oshima, J. Pancin, C. Papachristodoulou, C. Papadopoulos, C. Paradela, N. Patronis, A. Pavlik, P. Pavlopoulos, L. Perrot, R. Plag, A. Plompen, A. Plukis, A. Poch, C. Pretel, J. Quesada, T. Rauscher, R. Reifarth, M. Rosetti, C. Rubbia, G. Rudolf, P. Rullhusen, J. Salgado, L. Sarchiapone, C. Stephan, G. Tagliente, J. L. Tain, L. Tassan-Got, L. Tavora, G. Vannini, P. Vaz, A. Ventura, D. Villamarin, M. C. Vincente, V. Vlachoudis, R. Vlastou, F. Voss, H. Wendler, M. Wiescher, The N Tof Collaboration, Phys. Rev. Lett. **93** (2004) 161103.

[9] K. Wisshak, F. Voss, F. Käppeler, M. Krtička, S. Raman, A. Mengoni, R. Gallino, Phys. Rev. C **73** (2006) 015802.

[10] S. Jaag, F. Käppeler, Phys. Rev. C **51** (1995) 3465.

[11] Z. Y. Bao, H. Beer, F. Käppeler, F. Voss, K. Wisshak, T. Rauscher, At. Data Nucl. Data Tables **76** (2000) 70.

[12] K. Sonnabend, P. Mohr, K. Vogt, A. Zilges, A. Mengoni, T. Rauscher, H. Beer, F. Käppeler, R. Gallino, Astrophys. J. **583** (2003) 506.

[13] P. Mohr, T. Shizuma, H. Ueda, S. Goko, A. Makinaga, K. Hara, T. Hayakawa, Y.-W. Lui, H. Ohgaki, H. Utsunomiya, Phys. Rev. C **69** (2004) 032801.

[14] T. Shizuma, H. Utsunomiya, P. Mohr, T. Hayakawa, S. Goko, A. Makinaga, H. Akimune, T. Yamagata, M. Ohta, H. Ohgaki, Y.-W. Lui, H. Toyokawa, A. Uritani, S. Goriely, Phys. Rev. C **72** (2005) 025808.

[15] A. Mengoni, AIP, 2005, Volume 769, (p. 1209–1212).

[16] D. L. Lambert, Astron. Astroph. Rev. **3** (1992) 201.

[17] M. Arnould, S. Goriely, Phys. Rep. **384** (2003) 1.

[18] H. Schatz, A. Aprahamian, J. Görres, M. Wiescher, T. Rauscher, J. Rembges, F.-K. Thielemann, B. Pfeiffer, P. Möller, K.-L. Kratz, H. Herndl, B. Brown, H. Rebel, Phys. Rep. **294** (1998) 167.

[19] C. Fröhlich, G. Martinez-Pinedo, M. Liebendörfer, F.-K. Thielemann, E. Bravo, W. Hix, K. Langanke, N. Zinner, Phys. Rev. Lett. **96** (2006) 142502.

[20] V. Costa, M. Rayet, R. A. Zappalà, M. Arnould, Astron. Astroph. **358** (2000) 67.

[21] A. Richter, Prog. Part. Nucl. Phys. **44** (2000) 3.

[22] P. Mohr, J. Enders, T. Hartmann, H. Kaiser, D. Schiesser, S. Schmitt, S. Volz, F. Wissel, A. Zilges, Nucl. Instr. and Meth. A **423** (1999) 480.

[23] K. Vogt, P. Mohr, M. Babilon, J. Enders, T. Hartmann, C. Hutter, T. Rauscher, S. Volz, A. Zilges, Phys. Rev. C **63** (2001) 055802.

[24] J. Hasper, S. Müller, D. Savran, L. Schnorrenberger, K. Sonnabend, A. Zilges, Phys. Rev. C **77** (2008) 015803.

[25] K. Sonnabend, K. Vogt, D. Galaviz, S. Müller, A. Zilges, Phys. Rev. C **70** (2004) 035802.

[26] T. Rauscher, NON-SMOKER$^{\text{WEB}}$, version last updated August 26, 2006, http://nucastro.org/nonsmoker.html.

[27] A. J. Koning, S. Hilaire, M. C. Duijvestijn, AIP, 2005, Volume 769, (p. 1154–1159).

[28] G. Rugel, I. Dillmann, T. Faestermann, M. Heil, F. Käppeler, K. Knie, G. Korschinek, W. Kutschera, M. Poutivtsev, A. Wallner, Nucl. Instr. and Meth. B **259** (2007) 683.

[29] H. R. Weller, M. W. Ahmed, Mod. Phys. Lett. A **18** (2003) 1569.

[30] H. Ohgaki, S. Sugiyama, T. Yamazaki, T. Mikado, M. Chiwaki, K. Yamada, R. Suzuki, T. Noguchi, T. Tomimasu, IEEE Trans. Nucl. Sci. **38** (1991) 386.

[31] K. Sonnabend, J. Hasper, S. Müller, N. Pietralla, D. Savran, L. Schnorrenberger, A. Zilges, AIP Conf. Proc. in press (2008).

[32] K. Lindenberg, *Design and Construction of the Low-Energy Photon Tagger NEPTUN*, Doctoral Thesis, Institut für Kernphysik, TU Darmstadt, 2007.

[33] M. Elvers, J. Hasper, S. Müller, D. Savran, L. Schnorrenberger, K. Sonnabend, A. Zilges, J. Phys. G **35** (2008) 014027.

[34] C. Nair, A. R. Junghans, M. Erhard, D. Bemmerer, R. Beyer, P. Crespo, E. Grosse, M. Fauth, K. Kosev, G. Rusev, K. D. Schilling, R. Schwengner, A. Wagner, J. Phys. G **35** (2008) 014036.

[35] T. Rauscher, Phys. Rev. C **73** (2006) 015804.

[36] W. Rapp, J. Gorres, M. Wiescher, H. Schatz, F. Kappeler, Astrophys. J. **653** (2006) 474.

[37] T. Aumann, Eur. Phys. Journal A **26** (2005) 441.

[38] K. Sonnabend, M. Babilon, J. Hasper, S. Müller, M. Zarza, A. Zilges, Eur. Phys. Journal A **27** (2006) 149.

[39] E. Erhard, A. R. Junghans, R. Beyer, E. Grosse, J. Klug, K. Kosev, C. Nair, N. Nankov, G. Rusev, K. D. Schilling, R. Schwengner, A. Wagner, Eur. Phys. Journal A **27** (2006) 135.

[40] G. Gyürky, G. G. Kiss, Z. Elekes, Z. Fülöp, E. Somorjai, A. Palumbo, J. Görres, H. Y. Lee, W. Rapp, M. Wiescher, N. Özkan, R. T. Güray, G. Efe, T. Rauscher, Phys. Rev. C **74** (2006) 025805.

[41] N. Özkan, G. Efe, R. T. Güray, A. Palumbo, J. Görres, H. Y. Lee, L. O. Lamm, W. Rapp, E. Stech, M. Wiescher, G. Gyürky, Z. Fülöp, E. Somorjai, Phys. Rev. C **75** (2007) 025801.

[42] W. Rapp, I. Dillmann, F. Käppeler, U. Giesen, H. Klein, T. Rauscher, D. Hentschel, S. Hilpp, Phys. Rev. C **78** (2008) 025804.

[43] I. Dillmann, M. Heil, F. Käppeler, T. Rauscher, F.-K. Thielemann, Phys. Rev. C **73** (2006) 015803.

PoS(NIC X)043